

NUMERICAL SIMULATION OF CRACK GROWTH USING EXTENDED FINITE ELEMENT METHOD

J. Elanchezhian¹, K. Arul², A. Thanikasalam³, A. Adinarayanan⁴

¹ Assistant Professor, Mechanical Engineering, Anand Institute of Higher Technology, Tamil Nadu, India

² Assistant Professor, Mechanical Engineering, Anand Institute of Higher Technology, Tamil Nadu, India

³ Assistant Professor, Mechanical Engineering, Anand Institute of Higher Technology, Tamil Nadu, India

⁴ Assistant Professor, Mechanical Engineering, Anand Institute of Higher Technology, Tamil Nadu, India

Abstract: The X-FEM attempts to improve computational challenges associated with mesh generation by not requiring the finite element mesh to conform to cracks, and in addition, provides using higher-order elements or special finite elements without significant changes in the formulation. The essence of the X-FEM lies in subdividing the model problem into two distinct parts: mesh generation for the geometric domain (cracks not included), and enriching the finite element approximation by additional functions that model the flaw(s) and other geometric entities. In the X-FEM there is no need for the remeshing, because the mesh is not changed as the crack growths and is completely independent of the location and geometry of the crack. The discontinuities across the crack are modeled by enrichment functions. In this presentation, the numerical simulation of 2D LEFM accomplished using the Extended Finite Element Method [XFEM] is discussed. XFEM has been recently accepted as a powerful tool for the numerical simulation of crack modelling in Fracture Mechanics. According to this approach a discontinuous function and the asymptotic crack-tip displacement functions are added to the conventional finite element formulation. These additional functions, commonly known as the enrichment functions are derived from the theoretical background of the problem. XFEM is used in the implementation of 2D static and crack propagation problems with plane stress condition. Various methods of XFEM are compared with each other and are found in good agreement with that of the benchmark solutions. Also problems on the plate with inclined edge cracks under tensile loading are investigated.

Key Words: crack inclination, XFEM, mode-I loading, VCCT, cohesive elements

I. INTRODUCTION

The structural integrity of components used in nuclear power plants and aero-applications are pushed to their limits through various kinds of damage. Small flaws/cracks in micro and macro levels originate in these components through various processes like welding, machining and loads acting on them. To predict the effect of these cracks, different techniques are utilised today. XFEM is rather a new technique that enables unique advantages over the other ones. Many researchers have made an attempt to analyse the limits and advantages of XFEM through many solvers and the comparison of different methods used to formulate XFEM. Nicolas Moes et al., [1] is one of the earliest forms of XFEM. The authors formulated a finite element method for crack without re-meshing using the enrichment functions and the results were validated using numerical experiments. K. Sharma et al. [2] investigated the application to elasto-plastic problems and found significant difference in the results of LEFM and EPFM. They used the interaction integral approach to determine the SIFs and the Von-Mises yield criterion. E. Giner et al. [3] considered the analysis of fretting fatigue problems using XFEM and concluded that accurate computations of SIFs are possible on relatively coarse meshes using this method. They also concluded that including the orientation of the crack becomes easier. Casey L. Richardson et al. [4] investigated the crack propagation in brittle materials. They introduced a general algorithm for cutting triangulated domains and a quadrature rule and concluded that the method is comparatively faster and accurate. Gordana Jovicic et al. [5] developed an in-house code to model crack and compared the solutions with literature values and found them to be similar. They described the crack by means of the position of the tip and level set of a vector valued mapping. Sachin Kumar et al. [6] simulated crack growth under mode-I loading using CTOA criterion and concluded that CTOD/CTOA is an effective criterion for modelling effective crack growth in ductile materials. They used a proposed CTOA criterion and compared the results with J-R criterion. Sukumar et al. [7] modelled a quasi-static crack growth using XFEM and in particular, the array-allocation for enriched degrees of freedom, use of geometric-based queries for carrying assembly procedure for the discrete equations discussed. They concluded that they revealed the relative ease by which discontinuous fields through the partition of unity framework can be incorporated within a standard finite element package. Sachin Kumar et al. [8] investigated a multi grid XFEM for the elasto-plastic simulation of bi-material interfacial cracks and concluded that the proposed approach provides excellent results and saves huge computation time. G. Bharadwaj et al. [9] examined the numerical simulation of bi-material interfacial crack problems using extended isogeometric analysis. They modelled the material discontinuity at the interface using signed distance function whereas Heaviside and asymptotic crack tip functions are used to model the crack and concluded that the SIF obtained using XIGA are in good comparison with XFEM. Somnath Battacharya et al. [10] investigated the fatigue crack growth

simulations of FGM plate under cyclic thermal load by XFEM and concluded that the fatigue life of the materials is reduced considerably when these discontinuities are simultaneously present in the domain.

II. NUMERICAL FORMULATION

2.1 Governing Equations

The governing equations of elasto-statics with internal discontinuities are briefly reviewed and the equilibrium equation [10] is given as

$$\nabla \cdot \sigma + b = 0 \text{ in } \Omega \quad (1)$$

where, σ is the Cauchy stress tensor and b is the body force per unit volume.

By applying Von-Mises yield criterion, the complete incremental stress-strain relation [11] is given as

$$d\varepsilon_{ij} = \frac{d\sigma'_{ij}}{2G} + \frac{(1-2\nu)}{E} \delta_{ij} d\sigma_{kk} + d\lambda \frac{\partial f}{\partial \sigma_{ij}} \quad (2)$$

In Eq. (2) first two terms indicates elastic strain increment while last term indicate plastic strain increment. Also the term $d\lambda$ is proportionality constant termed as the plastic multiplier.

$$f(\sigma) = K(k) \quad (3)$$

where, f is a function, K is a material parameter and k is hardening parameter. Rearranging Eq. (3), we get

$$F(\sigma, k) = f(\sigma) - K(k) \quad (4)$$

Differentiating Eq. (4) and using some definitions we write

$$a^T d\sigma - A d\lambda = 0 \text{ where } a^T = \frac{\partial F}{\partial \sigma} dk \text{ and } A = -\frac{1}{d\lambda} \frac{\partial F}{\partial k} dk \quad (5)$$

The vector a is termed as flow vector. Eq. (2) can be written as

$$d\varepsilon = [D]^{-1} d\sigma + d\lambda \frac{\partial f}{\partial \sigma} \text{ and } d\lambda = \frac{1}{[A + a^T D a]} a^T D d\varepsilon \quad (6)$$

where, D is the usual matrix of elastic constants and. An elasto-plastic incremental stress-strain relation is obtained as

$$d\sigma = D_{ep} d\varepsilon \text{ where } D_{ep} = D - \frac{d_D d_D^T}{A + d_D^T a} d_D^T = a^T D \quad (7)$$

Here the yield function and plastic potential function are identical (associative flow rule) thus the elasto-plastic constitutive matrix D becomes symmetric. However when yield function is different than plastic potential function (non-associative flow rule), the elasto-plastic constitutive matrix D_{ep} becomes non-symmetric.

2.2 XFEM Approximation for Cracks

For 2-D crack modeling, the enriched displacement trial and test approximation [10, 11] is written in general form as

$$u^h(x) = \sum_{i=1}^n N_i(x) \left[\bar{u}_i + \underbrace{H(x) a_i}_{i \in n_r} + \underbrace{\sum_{\alpha=1}^4 \beta_\alpha(x) b_i^\alpha}_{i \in n_A} \right] \quad (8)$$

where, u_i is a nodal displacement vector associated with the continuous part of the FE solution, a_i is the nodal enriched DOF associated with $H(x)$, and $H(x)$ is the discontinuous Heaviside function, defined for those elements, which are completely cut by the crack which takes the value +1 on one side and -1 on other side of discontinuity. n is the set of all

nodes in the mesh, n_r is the set of nodes of elements which are completely cut by the crack and n_A is the set of nodes of elements which are partially cut by the crack. b_i^a is the nodal enriched DOF vector associated with crack tip enrichment $\beta_a(x)$. $\beta_a(x)$ is the asymptotic crack tip enrichment functions and are defined as

$$\beta_a(x) = \{\beta_1, \beta_2, \beta_3, \beta_4\} = \left[r^k \cos \frac{\theta}{2}, r^k \sin \frac{\theta}{2}, r^k \cos \frac{\theta}{2} \sin \theta, r^k \sin \frac{\theta}{2} \sin \theta \right] \quad (9)$$

where r and θ are the local coordinates of the crack tip. For LEFM enrichment functions $k = 0.5$, and for EPFM enrichment functions $k = 1/1 + \eta$, where η is the hardening exponent that depends on material.

If x_i is the node of interest then Eq. (8) can be written as:

$$u^h(x) = \sum_{i=1}^n N_i(x) \left[\bar{u}_i + \underbrace{[H(x) - H(x_i)]a_i}_{i \in n_r} + \underbrace{\sum_{\alpha=1}^4 [\beta_\alpha(x) - \beta_\alpha(x_i)]b_i^\alpha}_{i \in n_A} \right] \quad (10)$$

In Eq. (10), the difference between the values of the enrichment function at the evaluation point (Gauss point in the present simulations) and nodal point is considered. This modification also preserves the partition of unity property of the shape function.

2.3 XFEM Formulation for a Crack

For a crack, the incremental matrices, K and f are obtained using approximation function [11] defined by Eq. (10) as

$$K_{ij}^e = \begin{bmatrix} K_{ij}^{uu} & K_{ij}^{ua} & K_{ij}^{ub} \\ K_{ij}^{au} & K_{ij}^{aa} & K_{ij}^{ab} \\ K_{ij}^{bu} & K_{ij}^{ba} & K_{ij}^{bb} \end{bmatrix} \quad (11)$$

$$f^h = \{f_i^u \ f_i^a \ f_i^{b1} \ f_i^{b2} \ f_i^{b3} \ f_i^{b4}\}^T \quad (12)$$

The sub-matrices and vectors that appear in the foregoing equations are given as:

$$K_{ij}^{rs} = \int (B_i^r)^T C B_j^s h d\Omega \text{ where, } r, s = u, a, b \quad (13)$$

$$f_i^u = \int_{\Omega^e} N_i b d\Omega + \int_{\Gamma_t} N_i \bar{t} d\Gamma \quad (14)$$

$$f_i^a = \int_{\Omega^e} N_i (H(x) - H(x_i)) b d\Omega + \int_{\Gamma_t} N_i (H(x) - H(x_i)) \bar{t} d\Gamma \quad (15)$$

$$f_i^{b\alpha} = \int_{\Omega^e} N_i \beta_\alpha((x) - (x_i)) b d\Omega + \int_{\Gamma_t} N_i ((x) - (x_i)) \bar{t} d\Gamma$$

$$\text{where } \alpha = 1, 2, 3, 4 \quad (16)$$

where N_i are finite element shape function, B_i^u, B_i^a, B_i^b and $B_i^{b\alpha}$ are the matrices of shape function derivatives.

2.4 Computation of Stress Intensity Factors

The interaction integral is an effective tool for extracting the mixed-mode SIFs [11]. For two independent equilibrium states of a cracked body, the interaction integral is given as

$$M^{(1,2)} = \int_A \left[\sigma_{ij}^{(1)} \frac{\partial u_i^{(2)}}{\partial X_1} + \sigma_{ij}^{(2)} \frac{\partial u_i^{(1)}}{\partial X_1} - W^{(1,2)} \delta_{1j} \right] \frac{\partial q}{\partial X_j} dA \quad (17)$$

where $W^{(1,2)}$ is the mutual strain energy

$$W^{(1,2)} = \frac{1}{2} (\sigma_{ij}^{(1)} \varepsilon_{ij}^{(2)} + \sigma_{ij}^{(2)} \varepsilon_{ij}^{(1)}) = \sigma_{ij}^{(1)} \varepsilon_{ij}^{(2)} = \sigma_{ij}^{(2)} \varepsilon_{ij}^{(1)} \quad (18)$$

and q is given by

$$q = \left[1 - \frac{2|x|}{c} \right] \left[1 - \frac{2|y|}{c} \right] \quad (19)$$

Using the Eq. (17), the SIF values calculated from following equation

$$M^{(1,2)} = \frac{2}{E'} (K_I^{(1)} K_I^{(2)} + K_{II}^{(1)} K_{II}^{(2)}) \quad (20)$$

2.5 Criteria for Crack Growth

The maximum principal stress criterion [12] postulates that the crack growth occurs in a direction perpendicular to the maximum principal stress. Thus, at each crack tip, the local direction of crack growth θ_c is determined by the condition that the local shear stress is zero, that is

$$K_I \sin \theta_c + K_{II} (3 \cos \theta_c - 1) = 0 \quad (21)$$

Solution of this equation gives

$$\theta_c = 2 \tan^{-1} \left(\frac{K_I - \sqrt{K_I^2 + 8K_{II}^2}}{4K_{II}} \right) \quad (22)$$

According to this criterion, the equivalent mode-I SIF is

$$K_{Ieq} = K_I \cos^3 \left(\frac{\theta_c}{2} \right) - 3K_{II} \cos^2 \left(\frac{\theta_c}{2} \right) \sin \left(\frac{\theta_c}{2} \right) \quad (23)$$

This equivalent stress intensity factor is useful in the unstable fracture criterion i.e. $K_{Ieq} < K_{IC}$ where, K_{IC} is the critical value of mode-I stress intensity factor.

III. NUMERICAL SIMULATION

3.1 Inclined Centre Crack Static

A rectangular plate of 100 mm × 200 mm with a centre crack of length $a = 30$ mm with 30 degree inclined with horizontal is taken for the simulation. The tensile load of $\sigma = 100$ N/mm² is applied at the top edge of the plate and bottom edge is constrained as shown in Figure 1. The material of the plate is assumed as homogeneous and isotropic with $E = 200\,000$ N/mm² and Poisson ratio 0.3. A uniform mesh of 30 by 60 nodes is used in this simulation.

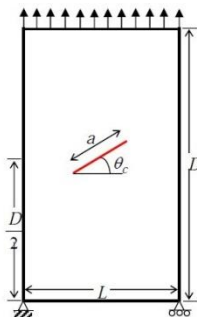


Fig. -1: Inclined Centre Crack

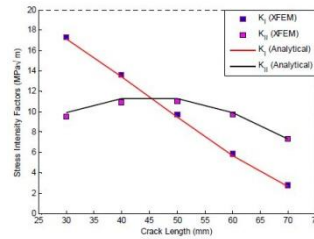


Fig. -2: Variation of SIF's with crack angle

Table 1 indicates values of SIF's for different crack angle from XFEM simulations and analytical results and there comparison shown in Figure 2. Analytical SIF's are calculated by [12]

$$K_{Analytical} = f\sigma\sqrt{\pi a} \quad (24)$$

where,

$$f = 1 + 0.128(a/L) - 0.288(a/L)^2 + 1.523(a/L)^3$$

$$K_{I(\theta_c)} = K_{I(0)} \cos^2(\theta_c) \quad (25)$$

$$K_{II(\theta_c)} = K_{I(0)} \cos(\theta_c) \sin(\theta_c) \quad (26)$$

where θ_c is crack angle with respect to horizontal.

Table -1: Variation of Mode-I and Mode-II stress intensity factors with crack inclination

Cra ck Ang le	K_I Ana lytic al	K_I XFE M	% Err or	K_{II} Ana lytic al	K_{II} XFE M	% Err or
30	17.1 536	17.3 090	- 0.90 5	9	9.54 25	3.64 7
40	13.4 215	13.6 290	- 1.54 6	11	10.9 280	2.96 5
50	9.44 99	9.70 51	- 2.70 0	11	11.0 407	1.96 5
60	5.71 7	5.88 01	- 2.83 8	9.90 36	9.73 83	1.66 9

3.2 Inclined Edge Crack Propagation (Quasi-static)

A rectangular plate of 100 mm × 200 mm with an edge crack of length $a_0 = 20$ mm with -40 degree inclined is taken for the simulation. The tensile load of $\sigma = 40$ N/mm is applied at the top edge of the plate and bottom edge is constrained as shown in Figure 3. The material of the plate is assumed as homogeneous and isotropic with $E = 74000$ N/mm² and Poisson ratio 0.3 [11]. A uniform mesh of 20 by 40 nodes is used in this simulation. Crack incremented by 2 mm after each step. Crack is propagated either crack length is 60 mm or K_{IC} less than K_{Ieq} .

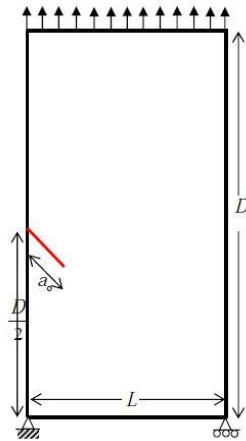


Fig. -3: Inclined Edge Crack

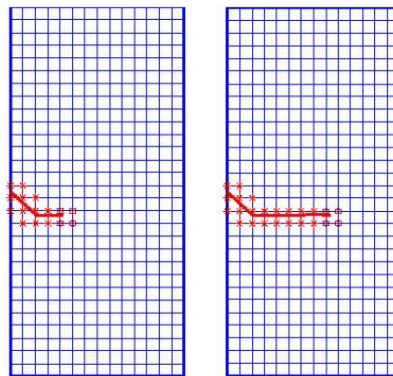


Fig. -4: XFEM Crack path for the edge crack

3.3 Edge Crack (Straight)

A plate with an edge crack of length $a = 30$ mm is taken for simulation. The tensile load of $\sigma = 200$ N/mm is applied at the top edge as shown in Figure 5. A uniform mesh of 30 by 60 nodes is used. The SIFs variation for LEFM and EPFM against crack length is presented in Figure 6.

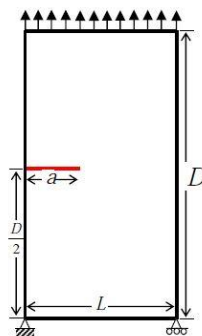


Fig. -5: Edge crack with dimensions

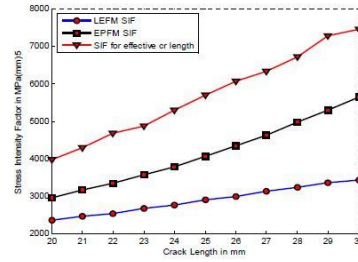


Fig. -6: Variation of SIF's with crack length

3.4 Inclined Centre Crack Propagation (Quasi-static)

A rectangular plate of 100 mm × 200 mm with a centre crack of length $a = 30$ mm with 30 degree inclined is taken for the simulation. The tensile load of $\sigma = 100$ N/mm is applied at the top edge of the plate and bottom edge is constrained. The material of the plate is assumed as homogeneous and isotropic with $E = 200\,000$ N/mm² and Poisson ratio 0.3. A uniform mesh of 30 by 60 nodes is used in this simulation. Crack incremented by 3 mm after each step. Crack is propagated either crack length is 50 mm or K_{IC} less than K_{Ieq} . Table 2 indicates the values of SIF's at left and right crack tip for inclined centre crack.

Table -2: The values of SIF's at left and right crack tip for inclined centre crack

Crack propagation step	K_{IL} XFEM	K_{ILL} XFEM	K_{Ieq} XFEM	θ_{CL}	K_{IR} XFEM	K_{ILL} XFEM	K_{Ieq} XFEM	θ_{CR}
I	17.31	9.54	23.03	-0.74	17.31	9.54	23.03	-0.74
II	22.41	5.08	24.00	0.41	22.41	5.09	24.01	0.41
III	23.99	4.13	25.05	0.33	24.00	4.22	25.06	0.33
IV	29.23	4.14	30.08	0.27	29.23	4.15	30.09	0.27
V	32.69	4.912	33.76	0.29	32.70	4.92	32.76	0.29
VI	36.35	4.84	37.29	0.26	36.35	4.85	37.29	0.26

IV. CONCLUSIONS

In this work, the analysis of static crack and crack growth problems has been carried out by XFEM. The crack is modeled by enrichment functions using regular finite element mesh. The values of SIFs are obtained using domain based interaction integral approach. From the results in third problems, it is clear that there is significant difference in the results of EPFM and LEFM. Moreover, these simulations show that XFEM can be easily extended to simulate elasto-plastic crack growth problems. During the analysis, it is also noticed that the XFEM can easily and accurately simulate crack growth problems, thus it can be easily extended to 3-D simulation.

REFERENCES

- [1]. Nicolas Moes, John Dolbow, Ted Belytschko, A finite element method for crack growth without remeshing, *Journal for Numerical Methods in Engineering* 46 (1999), p 131-150.
- [2]. E. Giner, N. Sukumar, F.D. Denia, F.J. Fuenmayor, Extended Finite Element Method For Fretting Fatigue Crack Propagation, *Journal of Solids and Structures* 29 (2008), p 251–260.
- [3]. Casey L. Richardson, Jan Hegemann, Eftychios Sifakis, Jeffry Hellrung, Joseph M. Teran, An XFEM Method for modelling geometrically elaborate cracks propagation in brittle materials, *Journal for Numerical Methods in Engineering* 18 (2009), p 45-71.
- [4]. Gordana Jovicic, Miroslav Zivkovic, Nebojsa Jovicic, Numerical Simulation of Crack Modeling using Extended Finite Element Method, *Journal of Mechanical Engineering* 55 (2009), p 216 - 218.
- [5]. Sachin Kumar, I.V. Singh, B.K. Mishra, Ductile Crack Growth Simulations under Mode-I Loading using CTOA Criterion, *Proceedings of International conference on structural integrity* (2014), p 217-223.
- [6]. N. Sukumar, J.-H. Prevost, Modeling quasi-static crack growth with the extended finite element method Part I Computer implementation, *Journal of Solids and Structures* 40 (2009), 7513-7537.
- [7]. Sachin Kumar, I.V. Singh, B.K. Mishra, R. Cardoso, J.W. Yoon, A multigrid XFEM for the elasto-plastic simulation of bi-material interfacial cracks, *Proceedings of International conference on structural integrity* (2014), p 642-649.
- [8]. G. Bharadwaj, I.V. Singh, B.K. Mishra, Numerical Simulation of Bi-material Interfacial Crack Problems Using Extended Isogeometric Analysis, *Proceedings of International conference on structural integrity* (2014), p 634-641.
- [9]. Somnath Bhattacharya, Kamal Sharma, Fatigue Crack Growth Simulations of FGM Plate Under Cyclic Thermal Load by XFEM, *Proceedings of International conference on structural integrity* (2014), p 1451-1455.
- [10]. N. Moes, J. Dolbow and T. Belytschko, A finite element method for crack growth without remeshing, *International Journal for Numerical Methods in Engineering*, 46, 131–50, (1999).
- [11]. I. V. Singh, B.K. Mishra, S. Bhattacharya and R. U. Patil, The numerical simulation of fatigue crack growth using extended finite element method, *International Journal of Fatigue*, 36, 109-119, (2012).
- [12]. M. Duflot and H.N. Dang, Fatigue crack growth analysis by an enriched meshless method, *Journal of Computational and Applied Mathematics*, 168, 155–64, (2004).